Coastal Engineering 112 (2016) 9–16

Contents lists available at ScienceDirect

Coastal Engineering

journal homepage: www.elsevier.com/locate/coastaleng

Shoreline change caused by the increase in wave transmission over a submerged breakwater due to sea level rise and land subsidence

Y. Kuriyama *, M. Banno [1]

Port and Airport Research Institute, Nagase 3-1-1, Yokosuka, Kanagawa 239-0826, Japan

ARTICLE INFO

Article history:
Received 20 October 2015
Received in revised form 3 January 2016
Accepted 20 February 2016
Available online xxxx

Keywords:
Low-crested breakwater
Climate change
Foreshore
Beachface
Beach erosion
Coral reef

ABSTRACT

Sandy beaches protected by submerged breakwaters, which have crests below sea level, are assumed to be vulnerable to relative sea level rise (SLR). In this study, the shoreline change due to sea level change and land subsidence along the Niigata West coast in Japan, which is protected by submerged breakwaters, was investigated using field data and a shoreline prediction model assuming that the shoreline change is caused by cross-shore sediment transport. The shoreline movement in the past 10 years was not directly caused by sea level change and land subsidence. However, our model predicts that over the next 100 years, the shoreline will retreat 60 m owing to the increase in the energy flux of incoming waves over the breakwater caused by SLR and land subsidence. These results imply that other sandy beaches protected by low-crested breakwaters as well as those behind coral reefs, which are natural submerged breakwaters, would experience non-negligible erosions caused by future relative SLR.

1. Introduction

Many sandy beaches in the world globally are eroding because of various natural and anthropogenic causes including reduced sediment supply from rivers and unbalanced longshore sediment transport rates around coastal structures. Countermeasures against beach erosion are classified into soft solution, which includes beach nourishment and sand bypassing, and hard solution, which includes groins, detached breakwaters, and submerged breakwaters (Komar, 1998).

Unlike detached breakwaters, submerged breakwaters do not interfere with the view of the horizon from the shore; therefore, submerged breakwaters are sometimes constructed as countermeasures against beach erosion where the availability of sediments for nourishment is limited and tourism is prevalent. However, because the crests of submerged breakwaters are below sea level, projected sea level rise (SLR) and land subsidence will lead to decreased wave energy dissipation by submerged breakwaters, causing instability in the sandy beaches. Thus, sandy beaches behind submerged breakwaters are vulnerable to SLR and land subsidence.

Moreover, whether a sandy beach is protected with coastal structures or not, according to the Bruun Rule (Bruun, 1962), the shoreline of the beach is expected to retreat owing to the seaward sediment transport caused by the upward and shoreward shift of the equilibrium beach profile due to relative SLR. Using long-term data of shoreline position and sea level along the East Coast of the USA, Zhang et al. (2004) showed that the rate of shoreline retreat is highly correlated with that of SLR. List et al. (1997), on the other hand, reported that along the Louisiana coasts, USA, no correlation was found between the amount of shoreline retreat estimated by the Bruun Rule and that of SLR. This suggests that the SLR-induced shoreline change is caused by the mechanism assumed in the Bruun Rule as well as other mechanisms including sediment transport to/from dunes and offshore regions as suggested by Stive (2004); Davidson-Arnott (2005) and others.

To predict shoreline changes caused by SLR, Karambas (2003) calculated the amount of shoreline retreat induced by several values of SLR ranging from 0.25 to 1.0 m using a process-based one-dimensional model, which predicts beach profile change by estimating the cross-shore variation of cross-shore sediment transport rate and was validated against experimental data. Cowell et al. (2006) estimated the probabilities of the amount of future shoreline changes on the Manly and Mission beaches in Australia using a profile translation model. Ranasinghe et al. (2012) developed a shoreline prediction model that calculates the dune erosion caused by wave run-up and stochastically predicted the amount of shoreline change by 2100 on Narrabeen Beach in Australia using storm time series that were probabilistically produced. Future shoreline changes from 2008 to 2095 on the Hasaki coast in Japan facing the Pacific Ocean were estimated by Banno and Kuriyama (2014) using their shoreline prediction model and considering SLR and wave climate change under two scenarios.

While a number of studies investigated the impact of SLR on natural beaches, research on the effect of SLR on beaches protected by coastal

* Corresponding author. Tel.: +81 46 844 5013; fax: +81 46 844 1274.
E-mail addresses: kuriyama@pari.go.jp (Y. Kuriyama), banno-m@pari.go.jp (M. Banno).
[1] Tel.: +81 46 844 5045; fax: +81 46 844 1274.

http://dx.doi.org/10.1016/j.coastaleng.2016.02.003
0378-3839/

structures including submerged breakwaters is rare. Yet even when coastal structures successfully protect the beaches behind them as expected, these beaches that were subjected to erosion in the past may still be at risk of erosion. Hence, examining shoreline changes caused by relative SLR on a sandy beach protected by submerged breakwaters can provide important information for beach conservation strategies. Moreover, the investigation results may also be helpful for preserving healthy beaches behind coral reefs, which form natural submerged breakwaters.

The objective of this study is to predict the future shoreline change caused by SLR and land subsidence along the Niigata West coast in Japan, which is protected by submerged breakwaters and is now experiencing land subsidence. First, the influences of sea level change and land subsidence on the shoreline change during the 10-year period from 2001 to 2011 is investigated. Then, the future shoreline change during the 100-year period from 2011 to 2111 is predicted using a shoreline prediction model.

2. Study site

2.1. Outline of the Niigata West coast

The Niigata West coast is located in central Japan and faces the Sea of Japan (Fig. 1). The coast was developed by the sediments that were discharged from the Shinano River and transported by the predominant westward longshore current. Because of the decrease in sediment discharge and the interruption of longshore sediment transport caused by river improvement (1875–1903), jetty construction (1987–1924) and openings of Ohkouzu and Sekiya diversion channels (1922 and 1972, respectively), the study coast as well as the coasts west of the study site suffered beach erosion since the 1910s (e.g., Kuriyama et al., 2006). In an effort to stop the erosion, detached breakwaters were constructed since the 1950s. Although they have protected the beaches behind them, erosion seaward of the breakwaters continued.

To prevent the offshore erosion, submerged breakwaters were constructed since 1989 approximately 350 m offshore of the detached breakwaters (Fig. 2). The cross-shore width of the submerged breakwaters is 40 m, and the crown height is approximately 2.5 m below the low water level. In addition to the submerged breakwaters, groins were also

Fig. 1. Map of Japan showing the location of the investigation site.

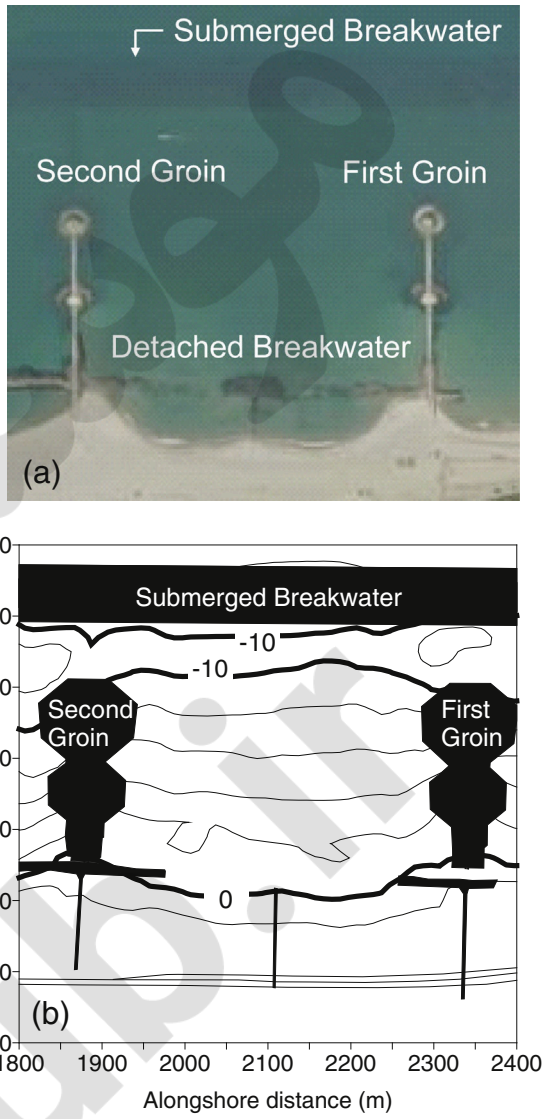

Fig. 2. (a) Aerial photograph taken in November 2007 and (b) morphology in July 2011 in the investigation area. Contours (m) are drawn at 2-m intervals in panel (b).

constructed since 1988 to reduce the alongshore current velocity shoreward of the submerged breakwaters.

The investigation area lies between the two groins shown in Fig. 2. A total of 200 m of previously constructed detached breakwaters was removed in 1995 and 1996. In 1996, a submerged groin with a crest height of 4.9 m below the low water level was constructed between the tip of the second groin and the submerged breakwater. A beach nourishment of 427,000 m^3 of sand was implemented during 1994–2000. Detailed information on the beach nourishment and coastal structure construction is shown in Kuriyama et al. (2006).

The median sediment diameter in the foreshore of the investigation area was 0.15–0.30 mm according to field surveys on sediment size conducted once a year from 2003 to 2011.

2.2. Morphological change

Based on the morphological data obtained approximately twice a year, the shoreline position defined at $z = 0.5$ m (z is the elevation according to the datum level) averaged alongshore in the investigation area moved shoreward from 2001 to 2007, and has been stable since 2007 (Fig. 3(a)). Because the investigation area was surrounded by the two groins extending to where the elevation was about −10 m

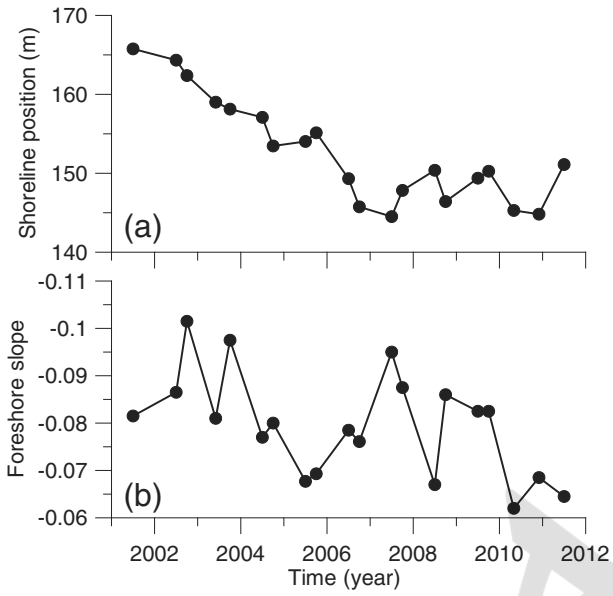

Fig. 3. (a) Shoreline position and (b) foreshore slope from 2001 to 2012. The shoreline position was defined to be positive in the seaward direction. The vertical axis in panel (b) is reversed. The negative beach slope indicates that the water depth increases as the seaward distance increases.

(Fig. 2(b)), the shoreline change was mainly caused by the cross-shore sediment transport.

The temporal variation of the foreshore slope, which is the mean slope at $z = 0$–1 m, indicates that the foreshore gradient decreased from 2001 to 2011, roughly corresponding to the shoreline change (Fig. 3(b)).

During the period from 2001 to 2007, when the shoreline retreated, the area seaward of the foreshore was also eroded (Fig. 4). However, during the period from 2007 to 2011, when the shoreline was stable, the morphological change in the area was relatively small.

2.3. Waves

Offshore waves were observed from 2001 to 2011 at a water depth of 35 m off Niigata West Port. Any missing data were substituted using the data obtained off Naoetsu Port, located 110 km west of Niigata West Port and the relationships between the significant wave heights

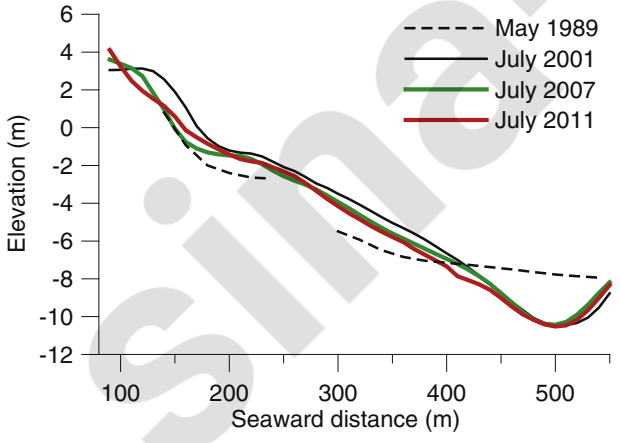

Fig. 4. Beach profiles averaged alongshore in the study area in 1989, 2001, 2007, and 2011. At the gap of the profile in 1989, where the seaward distance is 250 to 290 m, the previously constructed detached breakwater was located.

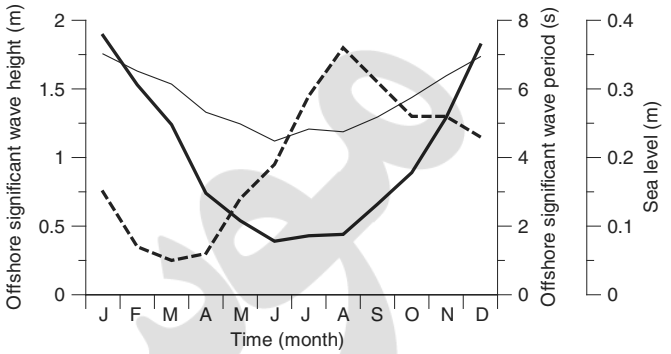

Fig. 5. Monthly averaged offshore significant wave height (thick solid line) and period (thin solid line) and sea level (broken line).

and periods at the two sites, which were estimated using the data from 2001 to 2009 (Kuriyama et al., 2013).

The seasonal variations in the monthly averaged offshore significant wave height and period show considerable changes in the wave conditions over the year (Fig. 5). The wave height and period are larger than 1.5 m and 6 s, respectively, from November to March, but smaller than 0.5 m and 5 s from June to August. Compared to the variations of the monthly averaged wave height and period, those of the yearly averaged values were small (Fig. 6). The standard deviations in yearly averaged wave height and period were 0.0543 m and 0.160 s, respectively.

2.4. Sea level

The sea levels were measured from 2001 to 2011 in Niigata West Port. The land subsidence values (Section 2.5) were removed from the measured values. Then, missing data were substituted using the astronomical tides predicted with the 60 component tides and the tidal harmonic constants estimated by the Japan Coast Guard (1992). Because sea levels vary according to atmospheric pressures, winds, waves, and ocean currents, and these effects are not included in the tide prediction, the means of the differences between the measured sea levels and the predicted tides averaged during 24 h before and after the period of missing data were added to the predicted values in the substitution.

The high, mean, and low water levels based on tide data from 2006 to 2010 are 0.422, 0.202, and −0.039 m, respectively. The monthly averaged sea level is highest in August, 0.36 m, and lowest in March, 0.05 m (Fig. 5). The average change rate of the yearly averaged sea level from 2001 to 2011, which was estimated using the linear least-squares method, was 0.0942 mm/year (Fig. 7).

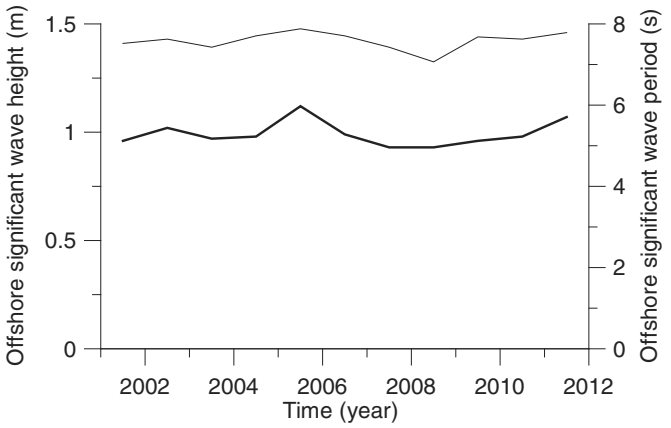

Fig. 6. Yearly averaged offshore significant wave height (thick line) and period (thin line).

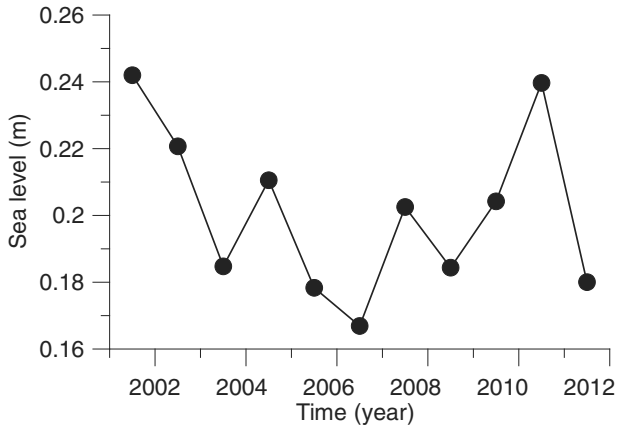

Fig. 7. Yearly averaged sea level from 2001 to 2012.

2.5. Land subsidence

During the 1950s, the land in the Niigata region subsided heavily, with a maximum subsidence rate of 0.54 m/year (e.g., Kaneko et al., 2007), mainly owing to groundwater extraction. After groundwater regulations were tightened, the subsidence rate decreased, but the land in and around the investigation site is still subsiding.

The amount of land subsidence on the Niigata West coast was estimated by the elevation change of the tidal gauge in Niigata West Port, surveyed once a year since 1997. The average land subsidence rate during 1997–2011 was 13.0 mm/year (Fig. 8).

3. Methods

3.1. Simulation model for shoreline change

The shoreline prediction model used in this study is based on the models developed by Kuriyama et al. (2012, 2013) which assume that the shoreline change is caused by cross-shore sediment transport and that the shoreline change rate is a function of the offshore wave energy flux E_f ($=\rho g H_{1/3,0}^2 C_g/16$; where ρ is the seawater density, g is the gravitational acceleration, $H_{1/3,0}$ is the offshore significant wave height, and C_g is the group velocity corresponding to the offshore significant wave period) taking into account the wave energy dissipation due to the submerged breakwater. The shoreline change rate was also assumed to be negatively proportional to the shoreline position y_s according to Katoh and Yanagishima (1988) and Miller and Dean (2004). The seaward shoreline change rate (the rate of shoreline advance) is enhanced by a more retreated shoreline position but suppressed by a more advanced one.

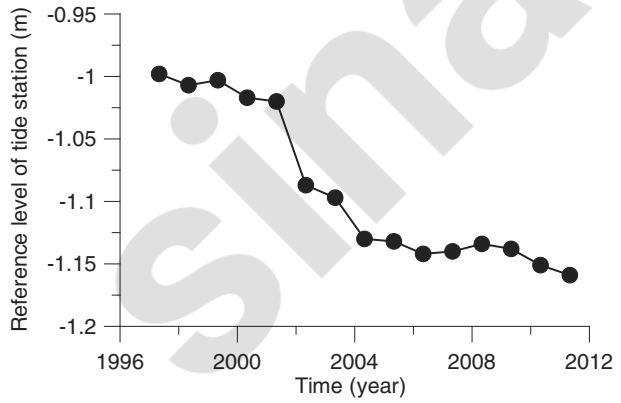

Fig. 8. Reference level of the tide station from 1997 to 2012.

In the present model, the change rates of the mean sea level and land subsidence were incorporated as expressed by Eq. (2).

$$y_{s,i} = y_{s,0} + \sum_{j=1}^{i} \left(\frac{dy_s}{dt}\right)_j \Delta t \tag{1}$$

$$\left(\frac{dy_s}{dt}\right)_j = a_0 + a_1 + a_2 E_j^2 + a_3 E_j + a_4 y_{s,j-1} + a_5 \left(\frac{d\overline{\eta}_j}{dt} - \frac{dz_{r,j}}{dt}\right) \tag{2}$$

where t is the time, a_0 is the geometrically obtained shoreline change rate due to land subsidence, i.e., $a_0 =$ (amount of land subsidence)/(foreshore slope), a_1 to a_5 are coefficients, $\overline{\eta}$ is the time-averaged sea level, and z_r is the elevation of a reference point for land subsidence measurement. The subscript j indicates the number of time steps.

The offshore wave heights considering the effects of the submerged breakwater were estimated through the wave transformation calculation over the submerged breakwater based on the model developed by Kuriyama (2010), which estimates the cross-shore variation of root-mean-square wave height assuming that the wave height probability density function has a Rayleigh distribution. The details of the model are described in the Appendix A. The estimated significant wave heights 150 m shoreward of the submerged breakwater ($z = -8.8$ m) were transformed to the offshore values using the shoaling coefficients, which were estimated using the water depth and wave length. The offshore wave heights considering the effects of the submerged breakwater were smaller than the original values by 13% for all waves and by 43% for waves larger than 2.0 m on the average during the period from 2001 to 2011.

3.2. Influences of sea level rise and land subsidence on the shoreline change

To examine the influences of sea level change and land subsidence on shoreline change in the past, two models with and without the terms related to the two factors of Eq. (2), the sixth and seventh terms on the right-hand side, were applied to the shoreline change data of July 2001 to July 2011. Because the waves and sea levels have strong seasonal variations (Fig. 5), the time interval of the shoreline change prediction was set at 3 months starting from 1 June. For the prediction, E_f was averaged for 3-month periods: June–August, September–November, December–February, and March–May. The $d\overline{\eta}/dt$ values were estimated using the two $\overline{\eta}$ values at the beginning and end of each 3-month interval, which were also averaged for 3 months. The values of dz_r/dt were based on the z_r values at the beginning and end of each 3-month interval. The beach profile used for the wave transformation calculation was based on averaged data from 2001 to 2008.

To judge which model is more appropriate to predict the shoreline change at the investigation site, the AIC values (Akaike, 1973) were estimated and compared. An AIC value is an estimate of the mean expected log likelihood of a model (Akaike, 1973; Sakamoto et al., 1986). The model with the minimum AIC value is considered to be the most appropriate model. The free parameter values, a_1 to a_5, were determined using the field data mentioned above during the period from 2001 to 2011 and the SCE-UA algorithm (Duan et al., 1993) so that the error between the shoreline positions measured and predicted was minimal. The predicted values when the topography was measured were estimated by interpolating the values at the three-month time intervals.

3.3. Prediction of future shoreline change affected by sea level rise and land subsidence

The shoreline change during the 100-year period from July 2011 to June 2111 was predicted using the most appropriate model with SLR and land subsidence, with only land subsidence and without SLR and land subsidence.

Table 1
AIC and best parameter values for Eq. (2) with and without the terms related to SLR and land subsidence.

	AIC	a_1 (m/day)	a_2 (s^2m)/(N^2day)	a_3 (sm)/(Nday)	a_4 (1/day)	a_5
Eq. (2) with the terms	94.1	9.63×10^{-2}	-1.28×10^{-9}	-2.66×10^{-11}	-5.64×10^{-4}	20.2
Eq. (2) without the terms	93.8	8.75×10^{-2}	-1.40×10^{-9}	-2.45×10^{-11}	-4.90×10^{-4}	–

The sea levels used in the prediction were estimated as the summation of the long-term and short-term sea level variations. The short-term one was estimated by removing the 1-year-moving-average values from the sea levels measured from July 2001 to June 2011, and repeated 10 times during the 100-year prediction period.

The long-term variation was assumed to be a quadratic function of time. The initial value was set at 0.198 m, which was the mean sea level during 2001 to 2011. The amount of sea level rise during the 100-year period was set at 0.74 m, which equals the amount of predicted sea level rise from 1986–2005 to 2100 under the RCP8.5 scenario (Church et al., 2013). The initial change rate of sea level rise was assumed to be 3.55 mm/year, which is the mean value at Japanese coasts along the Sea of Japan estimated based on sea levels measured during 2003–2010 (Miura and Kawamoto, 2013).

The amount of subsidence was set at 13.0 mm/year, which is the mean value for 2001–2011 as mentioned in Section 2.5.

The offshore wave heights taking into account the wave energy dissipation due to the submerged breakwater were estimated using the wave transformation model mentioned in Section 3.1 with the offshore significant wave heights and periods measured from 2001 to 2011, repeated 10 times during the prediction period, and the predicted values of sea level and land subsidence. First, the values every 2 h were estimated through the numerical simulations, and then the 3-month-average values, which were the input data for the shoreline change prediction, were estimated. The beach profile was the same as that used in Section 3.2.

Due to increase in tropical cyclone intensity caused by global climate change, wave climate is expected to change. Although influences of the wave climate change on bathymetry changes were examined by Ruggiero (2013); Kuriyama and Banno (2013); Banno and Kuriyama (2014) and others, the changes of mean and extreme wave heights during the next 100 years along the Japanese coasts facing the Sea of Japan, which include the study site, are expected to be small (e.g., Hemer et al., 2013; Shimura, 2015). Hence, the wave climate change was not considered in this study.

4. Results

4.1. Influences of sea level change and land subsidence on the shoreline change

Two models were used for the examination; one model includes the direct effects of sea level change and land subsidence on shoreline change and the other does not. The difference between the AIC values for the two models is 0.3 (Table 1). According to Sakamoto et al. (1986), an AIC difference larger than 1 is significant. This indicates that the difference between the two models is not significant. The shoreline positions estimated using the two models agreed well with the measured values, which retreated from 2001 to 2007, but were stable from 2007 to 2011 (Fig. 9). According to Kuriyama et al. (2013), which applied Empirical Orthogonal Function analysis and a shoreline prediction model without the terms related to sea level change and land subsidence to the same dataset as that used in this study, the contributions of shoreline changes caused by the offshore wave energy flux and shoreline position were assumed to be approximately 70% and 10%, respectively.

Although the difference between the two models is not significant as mentioned above, the AIC value for the model without the terms related to the two factors of Eq. (2) is slightly smaller than that for the model that includes the terms (Table 1). Thus, the future shoreline change was predicted using the model without the terms. The direct influences of sea level change and land subsidence on shoreline change will be discussed later.

4.2. Prediction of future shoreline change affected by sea level rise and land subsidence

The means and standard deviations of the predicted shoreline position during the ten 10-year periods in Fig. 10 show that the shoreline will retreat 61 m by 2111 with SLR and land subsidence and the standard deviations will increase. Without SLR and land subsidence, the shoreline would retreat only 10 m and stabilize; with only land subsidence in place, the shoreline would retreat 42 m.

The shoreline positions shown in Fig. 10 are those of the contour line at $z = 0.5$ m. The actual shoreline position corresponding to the rising sea level in 2111 predicted with SLR and land subsidence is located 11 m landward of the predicted shoreline positions in Fig. 10, considering a 0.74-m SLR and a beach slope of 1:15.

5. Discussion

The difference between the two models (with and without the direct influences of sea level change and land subsidence on shoreline change) is not significant as mentioned in Section 4.1. This indicates that the influences of sea level change and land subsidence on shoreline change were smaller than the influences of wave energy flux and shoreline position. Furthermore, the a_5 value in Eq. (2), which is the coefficient for the terms related to sea level change and land subsidence, was positive, indicating that the shoreline advances as the sea level rises. This result is contrary to that predicted by the Bruun Rule, in which the shoreline retreats with sea level rise. The shoreline change induced by the difference between the sea level and groundwater level as suggested by Duncan (1964) may have been dominant; Duncan (1964) showed that the shoreline advances at flood tide, when the sea level rises and becomes higher than the groundwater level owing to infiltration, and that the shoreline retreats at ebb tide because of seepage. However, the time scale discussed in this study is different from that in Duncan (1964).

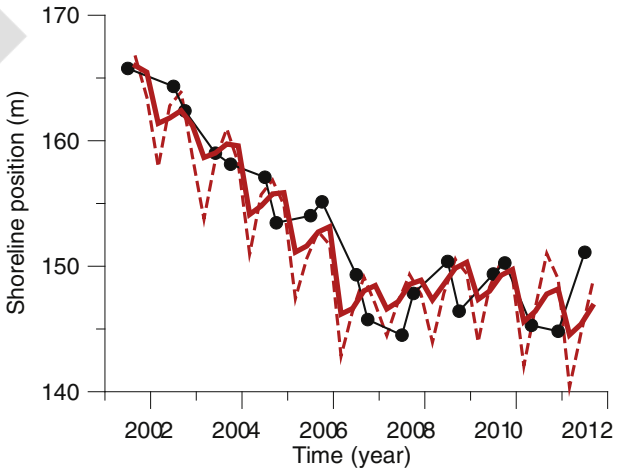

Fig. 9. Shoreline change measured (black solid circles and line) and predicted using Eq. (2) with (thin red broken line) and without (thick red solid line) the terms related to SLR and land subsidence.

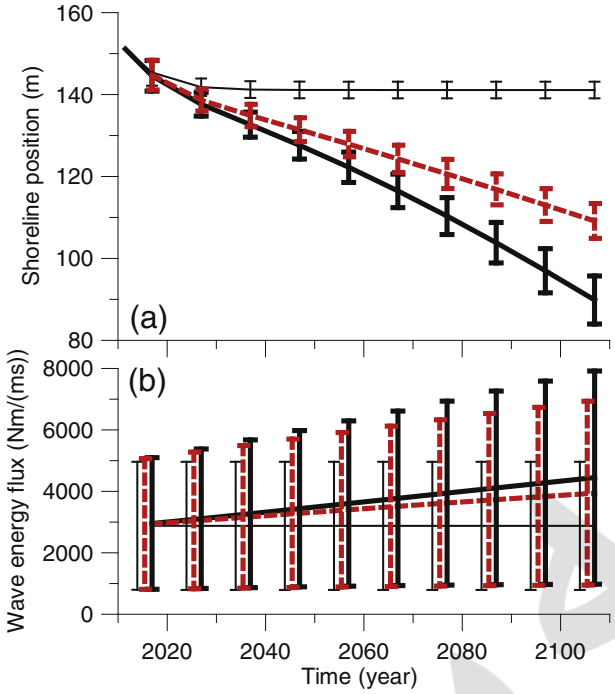

Fig. 10. (a) Shoreline change averaged for 10-year periods. Thick black solid, thick red broken, and thin black solid lines represent the values predicted with SLR and land subsidence, with land subsidence only, and without both, respectively. The vertical lines show the range of the mean ± 1 standard deviation. (b) The offshore wave energy flux estimated including the effect of the submerged breakwater. The symbols are the same as in panel (a).

The influences of sea level change and land subsidence need to be reexamined using more data.

The 61-m shoreline retreat predicted with SLR and land subsidence was caused by the increase in the energy flux of incoming waves over the submerged breakwater due to SLR and land subsidence. As the sea level rises and the land subsides, the distance between the sea level and the crest of the submerged breakwater increases, resulting in less wave breaking and less wave energy dissipation. The increase in the distance between the sea level and the breakwater crest from 2.5 to 4.5 m in 100 years results in a 55% increase in incoming wave energy flux. Even when only the land subsidence is taken into account, the distance increases from 2.5 to 3.8 m and the wave energy flux increases by 37%, resulting in a 42-m shoreline retreat.

The shoreline change behind a submerged breakwater is similar in many ways to that behind a coral reef. Coral reefs, which absorb wave energy and play a disaster-reduction role as natural submerged breakwaters, grow to keep pace with SLR. However, the growth rate of coral reefs does not necessarily match the rate of SLR (e.g., Woodroffe and Murray-Wallace, 2012; Woodroffe and Webster, 2014). Under such conditions, the beach behind may experience severe beach erosion.

6. Conclusions

The influences of sea level change and land subsidence on the shoreline change on the Niigata West coast in Japan, which is protected by submerged breakwaters, during the 10-year period from 2001 to 2011 were investigated using shoreline prediction models with and without the terms related to the two abovementioned factors. The results show that the influences were not statistically significant.

The future shoreline change during the 100-year period from 2011 to 2111 was predicted using the model without the terms related to the two factors. Although the shoreline movement was not directly caused by SLR and land subsidence, the increase in the energy flux of incoming waves over the submerged breakwater due to SLR and land subsidence led to a shoreline retreat of approximately 60 m by 2111.

The findings of this study were obtained based on data of a single sandy beach protected by a submerged breakwater. However, although the amount of beach erosion caused by SLR and land subsidence varies according to the grain size, the crown height of the submerged breakwater, and the offshore wave conditions, the findings suggest that sandy beaches around the world protected by low-crested breakwaters and coral reefs may experience non-negligible beach erosion owing to relative SLR, and that effective measures to mitigate the erosion should be investigated as suggested by Nicholls and Cazenave (2010).

Acknowledgments

The authors would like to thank two anonymous reviewers for their useful comments to improve the original manuscript. The field data were provided by the Niigata Port and Airport Construction Office and the Niigata Research and Engineering Office of the Port and Airport of the Hokuriku Regional Development Bureau and the Ports and Harbors Bureau, Ministry of Land, Infrastructure, Transport and Tourism, and the Marine Information Group of the Port and Airport Research Institute.

Appendix A. Wave transformation model

Outline of the model

The model estimates the cross-shore variation of the root-mean-square wave height H_{rms}. The wave height probability density function over the entire computational domain was assumed as to be a Rayleigh distribution, following Thornton and Guza (1983). The energy of waves with heights larger than the breaking wave height is dissipated.

The breaking wave height was estimated using Eq. (A1), as proposed by Seyama and Kimura (1988).

$$\frac{H_b}{h_b} = C_{br}\left[0.16\frac{L_0}{h_b}\left\{1-\exp\left[-0.8\pi\frac{h_b}{L_0}\left(1+15\tan^{4/3}\beta\right)\right]\right\}-0.96\tan\beta+0.2\right] \tag{A1}$$

where H_b is the breaking wave height, h_b is the breaking water depth, C_{br} is a nondimensional coefficient, L_0 is the offshore wavelength, and $\tan\beta$ is the beach slope. The nondimensional coefficient C_{br} was introduced by Kuriyama (1996) to fit experimental data-based Eq. (A1) to field data. The beach slope was defined as positive for water depth increasing seaward and estimated as the average slope in a 10-m-long region for which the definition point was located at the center.

Wave energy dissipation was estimated using the periodic bore model proposed by Thornton and Guza (1983) and 20 representative wave heights ranging from H_b to $3H_b$.

$$\frac{\partial E_w C_g \cos\theta}{\partial y} = \int_{H_b}^{\infty} P(H)B(H)dH$$
$$B(H) = \frac{1}{4}\rho g\frac{1}{T}\frac{(B_w H)^3}{h} \tag{A2}$$

where E_w is the wave energy, θ is the wave direction, y is the seaward distance, $P(H)$ is the probability density of the wave height, T is the wave period, H is the wave height, B_w is a nondimensional parameter, and h is the water depth.

The parameter B_w was formulated as in Eq. (A3) of Kuriyama and Ozaki (1996) using Seyama and Kimura's (1988) experimental data.

$$B_w = C_B\{1.6-0.12\ln(H_0/L_0)+0.28\ln(\tan\beta)\} \tag{A3}$$

where H_0 is the offshore wave height and C_B is a nondimensional coefficient.

The calculation used the peak wave period as the wave period, following Grasmeijer and Ruessink (2003). The significant wave height

$H_{1/3}$ was estimated as $H_{1/3} = 1.416\,H_{rms}$. The wave direction was assumed to be perpendicular to the shore.

Calibration of the model

The nondimensional coefficients, C_{br} in Eq. (A1) and C_B in Eq. (A3), were determined using wave data obtained seaward and shoreward of the submerged breakwater along the transect at the alongshore distance of 2100 m (Fig. 2) every 2 h during the period from 25 November 2008 to 25 February 2009. The measurement station seaward of the submerged breakwater Sta. 1 was located at the cross-shore distance of 1270 m ($z = -12.5$ m) and the two stations shoreward of the breakwater Sta. 2 and 3 were located at the cross-shore distances of 500 m and 375 m, respectively ($z = -8.8$ m and -4.6 m). The offshore boundary was set at Sta. 1, and the grid size was 5 m.

The obtained coefficients are $C_{br} = 0.55$ and $C_B = 0.50$. Although the model slightly over- and under-predicted the values when the wave height was smaller and larger than 1.5 m, respectively, the model agreed well with the measured data of significant wave heights shoreward of the submerged breakwater (Fig. A1); the average of the root-mean-square errors of the measured and predicted values at Sta. 2 and Sta. 3 was 0.151 m.

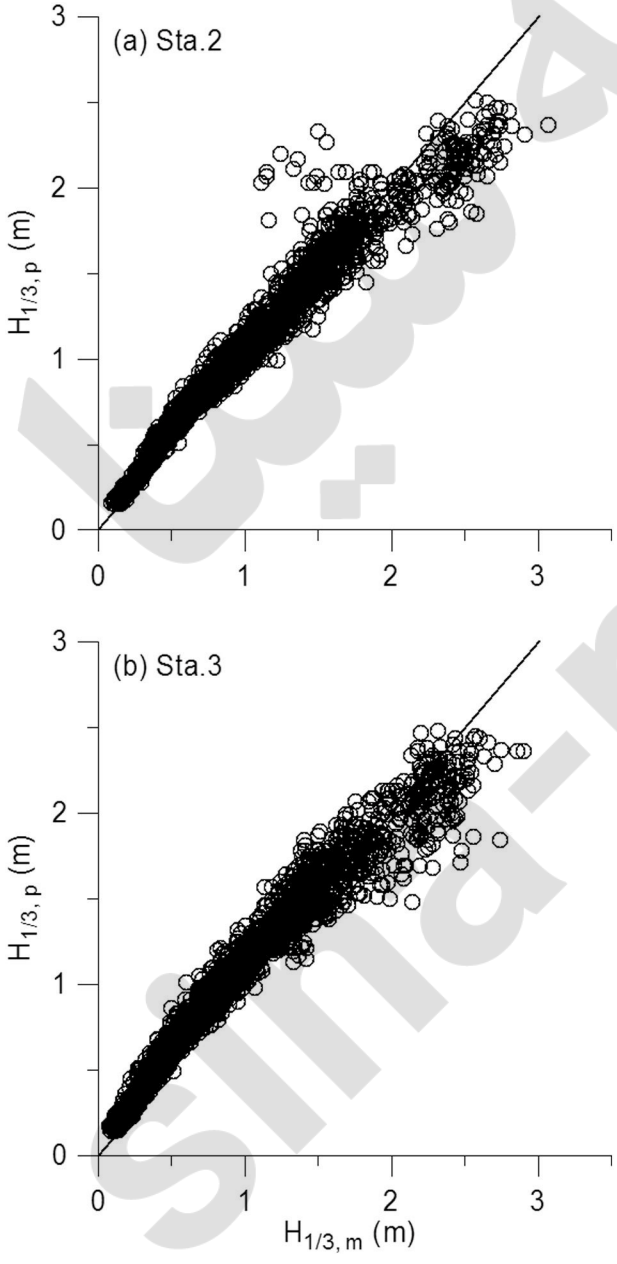

Fig. A1. Comparisons between the measured and predicted significant wave heights ($H_{1/3,m}$ and $H_{1/3,p}$) at Station 2 (a) and Station 3 (b). The solid lines represent $H_{1/3,p} = H_{1/3,m}$.

References

Akaike, H., 1973. Information theory and an extension of the maximum likelihood principle. In: Petrov, B.N., Csaki, F. (Eds.), Second International Symposium on Information Theory. Academiai Kiado, Budapest, Hungary, pp. 267–281.

Banno, M., Kuriyama, Y., 2014. Prediction of future shoreline change with sea-level rise and wave climate change at Hasaki, Japan. Coast. Eng. Proc. 1 (34). http://dx.doi.org/10.9753/icce.v34.sediment.56 (sediment.56).

Bruun, P., 1962. Sea level rise as a cause of shore erosion. J. Waterw. Harb. Div. 88 (1–3), 117–130.

Church, J.A., Clark, P.U., Cazenave, A., Gregory, J.M., Jevrejeva, S., Levermann, A., Merrifield, M.A., Milne, G.A., Nerem, R.S., Nunn, P.D., Payne, A.J., Pfeffer, W.T., Stammer, D., Unnikrishnan, A.S., 2013. Sea Level Change. In: Stocker, T.F., Qin, D., Plattner, G.-K., Tignor, M., Allen, S.K., Boschung, J., Nauels, A., Xia, Y., Bex, V., Midgley, P.M. (Eds.), Climate Change 2013: the Physical Science BasisContribution of Working Group I to the Fifth Assessment Report of the Intergovernmental Panel on Climate Change. Cambridge University Press, Cambridge, United Kingdom and New York, NY, USA.

Cowell, P.J., Thom, B.G., Jones, R.A., Everts, C.H., Simanovic, D., 2006. Management of uncertainties in predicting climate-change impacts on beaches. J. Coast. Res. 22, 232–245.

Davidson-Arnott, R.G.D., 2005. A conceptual model of the effects of sea level rise on sandy coasts. J. Coast. Res. 21 (6), 1166–1172.

Duan, Q.Y., Gupta, V.K., Sorooshian, S., 1993. Shuffled complex evolution approach for effective and efficient global minimization. J. Optim. Theory Appl. 73 (3), 501–521.

Duncan, J.R., 1964. The effects of water table and tidal cycle on swash-backwash sediment distribution and beach profile development. Mar. Geol. 2, 186–197.

Grasmeijer, B.T., Ruessink, B.G., 2003. Modeling of waves and currents in the nearshore parametric vs. probabilistic approach. Coast. Eng. 49, 185–207.

Hemer, M.A., Fan, Y., Mori, N., Semedo, A., Wang, X.L., 2013. Projected changes in wave climate from a multi-model ensemble. Nat. Clim. Chang. 3, 471–476. http://dx.doi.org/10.1038/nclimate1791.

Japan Coast Guard, 1992. Tidal Harmonic Constants Tables Japanese Coast. Pub. No. 742. Japan Hydrographic Association, Tokyo, Japan.

Kaneko, M., Kobayashi, T., Sekiya, K., Kitajima, E., 2007. Land subsidence in and around Niigata City after tightening regulations about the extraction of natural gas dissolved in water. Annual Rep. Niigata Prefectural Inst. of Public Health and Environmental Sciences 22. Niigata Prefectural Institute of Public Health and Environmental Sciences, Niigata, Japan, pp. 85–91 (in Japanese).

Karambas, T.V., 2003. Modeling of sea-level rise effects on cross-shore coastal erosion. J. Mar. Environ. Eng. 7, 15–24.

Katoh, K., Yanagishima, S., 1988. Predictive model for daily changes of shoreline. Proceedings of the 21st International Conf. Coastal Engineering. ASCE, New York, pp. 1253–1264.

Komar, P.D., 1998. Beach Processes and Sedimentation. second ed. Prentice Hall, Inc, New Jersey, USA.

Kuriyama, Y., 1996. Models of wave height and fraction of breaking waves on a barred beach. Proceedings of the 26th International Conf. Coastal Engineering. ASCE, New York, pp. 247–260.

Kuriyama, Y., 2010. A one-dimensional parametric model for undertow and longshore current velocities on barred beaches. Coast. Eng. J. 51 (2), 133–155. http://dx.doi.org/10.1142/S0578563410002130.

Kuriyama, Y., Banno, M., 2013. Numerical investigation of the influence of the enhancement of cyclones on long-term shoreline movement. Proceedings 12th International Coastal Symposium. J. Coast. Res. Spec. Issue 65, 1797–1802. http://dx.doi.org/10.2112/SI65-304.1.

Kuriyama, Y., Ozaki, Y., 1996. Wave height and fraction of breaking waves on a bar-trough beach-Field measurements at HORS and modeling-. Rep Port and Harbour Res Inst 35 (1). Port and Harbour Research Institute, Yokosuka, Japan, pp. 1–38.

Kuriyama, Y., Yamaguchi, S., Ikegami, M., Takano, S., Tanaka, J., 2006. Morphological changes around large-scale submerged breakwater on the Niigata coast, Japan. Proceedings of the 30th International Conf. Coastal Engineering. ASCE, New York, pp. 3695–3707.

Kuriyama, Y., Banno, M., Suzuki, T., 2012. Linkages among interannual variations of shoreline, wave and climate at Hasaki, Japan. Geophys. Res. Lett. 39, L06604. http://dx.doi.org/10.1029/2011GL050704.

Kuriyama, Y., Banno, M., Kishi, H., Satoh, T., Mizuuchi, K., 2013. Morphological change of nourished beach behind submerged breakwater of the Niigata coast. Proceedings of Coastal Dynamics 13. ASCE, New York, pp. 1015–1024.

List, J.H., Sallenger, A.H., Hansen, M.E., Jaffee, B.E., 1997. Accelerated relative sea-level rise and rapid coastal erosion: testing a causal relationship for the Louisiana barrier islands. Mar. Geol. 140, 347–363.

Miller, J.A., Dean, R.G., 2004. A simple new shoreline change model. Coast. Eng. 51, 531–556. http://dx.doi.org/10.1016/j.coastaleng.2004.05.006.

Miura, Y., Kawamoto, S., 2013. Analysis of sea level change with continuous GPS stations at tide gauges. J. Geospatial Information Authority of Japan, No 123. Geospatial Information Authority of Japan, Tsukuba, Japan, pp. 21–82 (in Japanese).

Nicholls, R.J., Cazenave, A., 2010. Sea-level rise and its impact on coastal zones. Science 328 (5985), 1517–1520. http://dx.doi.org/10.1126/science.1185782.

Ranasinghe, R., Callaghan, D., Stive, M.J.F., 2012. Estimating coastal recession due to sea level rise: beyond the bruun rule. Clim. Chang. 110, 561–574. http://dx.doi.org/10.1007/s10584-011-0107-8.

Ruggiero, P., 2013. Is the intensifying wave climate of the U.S. Pacific northwest increasing flooding and erosion risk faster than sea-level rise? J. Waterw. Port Coast. Ocean Eng. 139 (2), 88–97.

Sakamoto, Y., Ishiguro, M., Kitagawa, G., 1986. Akaike Information Criterion Statistics. D. Reidel Publishing Company, Dordrecht, the Netherlands and Tokyo, Japan.

Seyama, A., Kimura, A., 1988. The measured properties of irregular wave breaking and wave height change after breaking on the slope. Proceedings of the 21st International Conf. Coastal Engineering. ASCE, New York, pp. 419–432.

Shimura, T., 2015. Long Term Projection of Ocean Wave Climate and its Climatic Factors Dissertation Kyoto University.

Stive, M.J.F., 2004. How important is global warming for coastal regions? An editorial comment. Clim. Change 64, 27–39.

Thornton, E.B., Guza, R.T., 1983. Transformation of wave height distribution. J. Geophys. Res. 88 (C10), 5925–5938.

Woodroffe, C.D., Murray-Wallace, C.V., 2012. Sea-level rise and coastal change: the past as a guide to the future. Quat. Sci. Rev. 54, 4–11. http://dx.doi.org/10.1016/j.quascirev.2012.05.009.

Woodroffe, C.D., Webster, J.M., 2014. Coral reefs and sea-level change. Mar. Geol. 352, 248–267. http://dx.doi.org/10.1016/j.margeo.2013.12.006.

Zhang, K., Douglas, B.C., Leatherman, S.P., 2004. Global warming and coastal erosion. Clim. Chang. 64, 41–58.